Profiling multilayer structures with monoenergetic positrons

A. Vehanen, K. Saarinen, P. Hautojärvi, and H. Huomo
Laboratory of Physics, Helsinki University of Technology, 02150 Espoo, Finland
(Received 25 September 1986)

Variable-energy (0–25 keV) positron stopping and annihilation behavior is studied in a multilayer structure, which has subsequent (~3000-Å-thick) ZnS and Al_2O_3 layers on a glass substrate. Direct information on positron slowing-down properties is obtained. The positron implantation profile is shown to possess the shape of a derivative of a Gaussian function, in contrast to the more commonly used exponential profile. The mean positron penetration depth varies with incident positron energy E (in keV) as $\bar{z}=[4.0(3)\ \mu g/cm^2](E)^{1.62(5)}$. The feasibility of the present technique for depth profiling of heterogeneous samples is considered. The accuracy of determining the positions of the interfaces is typically less than 100 Å in the present system. The mobility of positrons in ZnS and Al_2O_3 layers is observed to be very low. This corresponds to positron trapping into structural defects with a relatively high concentration.

I. INTRODUCTION

The development of monoenergetic positron beams in recent years has enabled studies of surface properties, in particular, studies of atomic scale disorder at the surface and in the near-surface region. These measurements are based on a strong positron surface interaction, and on the capability of positron localization at open-volume lattice defects.[1,2] Various positron processes at and near the surface can be used for material characterization.[3,4] Recently the depth distribution of vacancy-type defects have been measured,[5,6] which is based on monitoring the energy-dependent fraction of positrons diffusing back to the surface.

Deeper areas of the sample can be probed by measuring properties of the annihilation radiation inside the sample, following monoenergetic positron injection. These data are obtained by measuring the shape of the Doppler-broadened 511-keV annihilation line versus incident positron energy E. Results in ion-implanted metals,[7–9] amorphous metals,[10] and semiconductors[11] have already been published. An attempt has also been made to couple the information from annihilation line-shape and positron back-diffusion measurements in the presence of an inhomogeneous defect distribution.[12]

For analysis of heterogeneous samples at deeper[5] ($\geq$200 Å) depths, proper knowledge on the positron implantation profile is essential. An exponential function has commonly been used,[1] although computer simulations indicate that the positron stopping profile has a shape close to a derivative of a Gaussian function.[13] From studies of positron behavior in multilayer structures with well-defined layer thicknesses, direct information on positron slowing-down properties can be obtained.

In this paper we measure the positronium (Ps) fraction[2] f and the annihilation line-shape parameter[14] S, as a function of the positron implantation energy E, in samples consisting of subsequent layers of Al_2O_3 and ZnS grown on a glass substrate. These data are analyzed to yield information on the positron implantation profile, as well as on the mobility of positrons within the layers. The depth resolution of the technique to probe heterostructures is finally discussed. The organization of the paper is as follows. Section II gives the experimental details, while Sec. III contains the data analysis. Results are presented and discussed in Sec. IV, and Sec. V concludes the paper.

II. EXPERIMENTAL PROCEDURE

The experiments were performed with a variable-energy positron beam in ultrahigh vacuum.[15] Using a 50-mCi ^{58}Co β^+ source and a backscattering W(110) moderator, the slow positron beam intensity was 7×10^5 sec^{-1}, corresponding to a moderation efficiency $\varepsilon=0.25\%$. The incident positron energy E was variable from 0 to 25 keV.

Positron annihilation spectra in the proximity of the sample were measured with a HP Ge detector (efficiency 35%) and data were acquired with a digitally stabilized multichannel analyzer system. We derived the positronium fraction f emitted from the sample from the shape of the measured γ spectra,[4,15] and detected the shape of the Doppler-broadened 511-keV annihilation line.[14] At each incident positron energy E, 1×10^5 and 4×10^6 counts were collected into the 511-keV annihilation line in the $f(E)$ and $S(E)$ measurements, respectively, with a rate of 7400 counts/sec.

The studied sample, obtained from Lohja Corporation, was used to fabricate electroluminescent display units. It consisted of a heterostructure, where a 3000-Å-thick Al_2O_3 layer was grown with an atomic layer epitaxy technique on a glass substrate, followed by a ZnS layer (4000 Å thick), and finally another similar 3000-Å-thick Al_2O_3 layer. The layer thicknesses had a typical accuracy of 150 Å. The crystalline structure was polycrystal with an average crystallite size of ~1000 Å.[16] The structure of the specimen is also shown in Fig. 1. We studied three separate cuts of the same sample (locations 1–3 in Fig. 1), where only one, two, or all three layers were present on the glass substrate, respectively. After ultrasonic cleaning, the samples were mounted into the UHV chamber.

Auger spectra showed that a thin impurity layer could be removed after sputtering with 500-eV Ar^+ ions. Positron measurements were performed before and after this sputtering.

III. DATA ANALYSIS

Since the positron mobility in all samples was measured to be relatively small (see below), we analyzed the experimental annihilation line-shape $S(E)$ data, neglecting positron diffusion effects. No positron reflection or transport at the interfaces was assumed. For each incident positron energy E, we calculated the line-shape parameter S, defined as the area of a fixed region in the center of the annihilation line divided by the total peak area.[14] Each layer in the sample was assumed to be homogeneous, and therefore the calculated value of $S(E)$ becomes a superposition of characteristic values S_i in each layer i, weighted with the probability η_i that the positrons will annihilate in layer i. In the limit of zero positron mobility, η_i is simply the fraction of positrons, which will thermalize in the ith layer after implantation.

The positron implantation profile $P(z,E)$ is taken as[13]

$$P(z,E)=-\frac{d}{dz}\left\{\exp\left[-\left[\frac{z-\delta_i}{z_{0i}}\right]^m\right]\right\}, \tag{1}$$

where

$$\bar{z}=z_{0i}\Gamma\left[1+\frac{1}{m}\right]=\frac{\alpha}{\rho_i}(E)^n \tag{2}$$

is the mean range of positrons at an implantation energy E (in keV). The parameter δ_i in each layer is simply determined from the condition that the positron transmission $T(z)=1-\int_0^z P(z,E)dz$ must be continuous at all values of z measured from the surface ($z=0$). Above, ρ_i is the material density and α ($=3.3\ldots4$ $\mu g/cm^2$), m ($=1\ldots2$), and n ($=1\ldots2$) are parameters which contain experimental[3,17] and theoretical[13] uncertainties.[18]

Consequently, the probability of positrons to thermalize and annihilate in the ith layer is

$$\eta_i(E)=\int_{a_i}^{b_i} P(z,E)dz\ , \tag{3}$$

where a_i and b_i are boundaries of layer i. Finally,

$$S(E)=\sum_i \eta_i S_i \tag{4}$$

can be compared to measured values of the line-shape parameter S at each incident energy E. This comparison can then be used to extract more accurate estimates for the parameters α, m, and n describing the implantation profile $P(z,E)$.

IV. RESULTS AND DISCUSSION

We measured the Ps fraction f versus incident positron energy E in each sample in the as-received state. The results are basically the same in all studied samples, with the diffusion parameter[3,4] $E_0 \leq 300$ eV. Light sputtering with Ar^+ ions did not change the curves, either. This may indicate that relatively strong positron trapping occurs in structural inhomogeneities present in each layer. Consequently, positron mobility in various layers would be very small. Similar phenomena were observed to occur in amorphous metals.[10] Another possibility is that thermal positrons diffusing back to the surface do not form Ps, while the observed Ps signal f is due to epithermal positrons,[19] which form positronium at the sample surface.[20,21] This can be tested with positron line-shape measurements presented below.

The measured line-shape parameter S as a function of the incident energy E is depicted in Fig. 2 in a sample containing a single Al_2O_3 layer on a glass substrate. The positron mobility is observed to be very low, as seen by a steep decrease of S at low E from the surface value $S_S=0.4152$ towards a value $S_A=0.3975$, which we adopt as a characteristic value for positrons annihilating in the Al_2O_3 layer. At $E>5$ keV, positrons start to "feel" the substrate material, and S levels to $S_G=0.4160$, describing annihilations in the glass substrate. The solid line in the upper horizontal axis corresponds to an energy E (see below), where the median positron penetration depth R crosses the Al_2O_3/glass interface.

We have fitted the data to Eqs. (1)–(4) with $\alpha=4$ $\mu g/cm^2$, $n=1.6$ (Refs. 13 and 17), and S_A and S_G as given above. With m as a parameter, Fig. 2 shows two fits, corresponding to exponential ($m=1$) and Gaussian ($m=2$) positron implantation profiles. We note that the exponential profile is not compatible with our data, whereas the $m=2$ curve matches with the data at all $E\geq3$ keV. The deviations at small E are due to positron motion to the surface, as mentioned earlier. This small diffusion has negligible effects at higher E, due to an increasing ratio of the positron implantation and diffusion ranges.

Figure 3 shows a similar plot in the sample with the ZnS/Al_2O_3/glass structure. Again, the data at small E describe positron motion to the surface. At $E\approx4$ keV, S reaches a level $S_Z=0.4300$ characteristic of the ZnS layer. The presence of the intermediate Al_2O_3 layer is seen as a

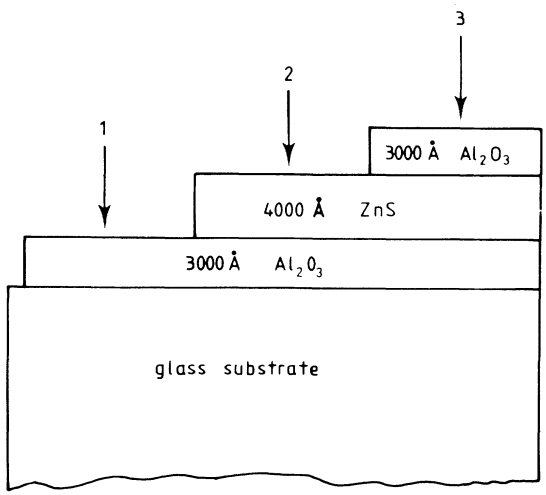

FIG. 1. Cross section of the studied multilayer specimen. Three different cuts of the same sample were studied with monoenergetic positrons, shown with arrows in the figure.

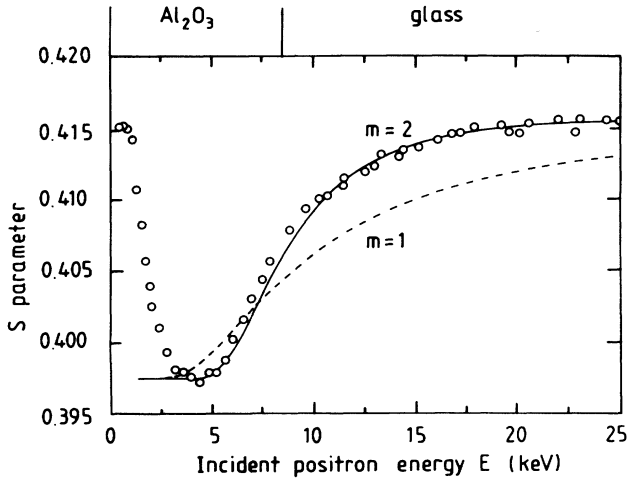

FIG. 2. Experimental (dots) and calculated (lines) values of the Doppler-broadened annihilation line-shape parameter S vs incident positron energy E in the sample with a 3000-Å-thick Al_2O_3 layer on a glass substrate. The two fits correspond to exponential ($m=1$) and Gaussian ($m=2$) positron implantation profiles with a mean penetration range $\bar{z} \propto E^n$, where $n=1.6$. The upper horizontal axis has a line at an energy E, where the median positron range R crosses the Al_2O_3/glass interface.

decrease in S at $E=7$ keV, followed by a shallow minimum around $E=13$ keV. Due to the increasing width of the positron implantation profile, the line-shape parameter S does not reach the level $S_A=0.3975$ any more, as the calculated fraction of positrons implanted in the Al_2O_3 layer has a maximum $\eta_{Al_2O_3,max}=0.35$ at 10 keV [Eq. (3)]. Finally, S levels towards $S_G=0.4160$. This is the same value, which was also observed at high E in Fig. 2.

The use of exponential ($m=1$) or Gaussian ($m=2$) implantation profiles produces calculated $S(E)$ curves shown in Fig. 3. Again the latter fits the data at $E \geq 4$ keV, whereas an exponential profile is far too wide to match with experiments. Figure 3 also demonstrates the effect of n on the calculated $S(E)$ curves. The three separate fits with $m=2$ correspond to $n=1.65$ (dotted line), $n=1.60$ (solid line), and $n=1.55$ (dashed-dotted line). The solid line with $n=1.60$ is seen to be the best choice of the three n values. It was also used in fitting the earlier data in Fig. 2.

Figure 4 shows measured and calculated $S(E)$ data in the Al_2O_3/ZnS/Al_2O_3/glass system. All parameters are now fixed to previous values (Figs. 2 and 3) with $n=1.60$. Again we notice a remarkably good agreement using a Gaussian-shaped positron implantation profile at $E>4$ keV, where diffusion of positrons in the present system can be neglected. The effect of each layer to $S(E)$ is seen in Fig. 4, although information becomes more and more convoluted at higher E, where the width of the implantation profile increases rapidly.

Unlike the situation in fitting the Ps fraction f versus E data,[21,22] the parameter m does not appear to be correlated with other implantation profile parameters n and α. This is valid for all three samples shown in Figs. 2–4. When α, n, and m are all allowed to vary in the fitting procedure, the statistical uncertainty in m is $\sigma_m=0.1$, and the best value is between $m=2.0$ and 2.1 in all cases. On the other hand, n and α are strongly correlated, with best values $n=1.62(1)$ and 1.72(1) using the extreme[13,17] values for $\alpha=4.0$ and 3.3 $\mu g/cm^2$, respectively. The best value for α is 4.0 $\mu g/cm^2$, and the goodness of the fit decreases rapidly outside $\alpha=4.0\pm0.3$ $\mu g/cm^2$. We conclude that the positron stopping profile is best described by a derivative of a Gaussian function, with a mean depth $\bar{z}=[4.0(3)\ \mu g/cm^2](E)^{1.62(5)}$. The corresponding relation for z_0 [Eqs. (1) and (2)] is $z_0=[4.5(4)\ \mu g/cm^2](E)^{1.62(5)}$, and for the

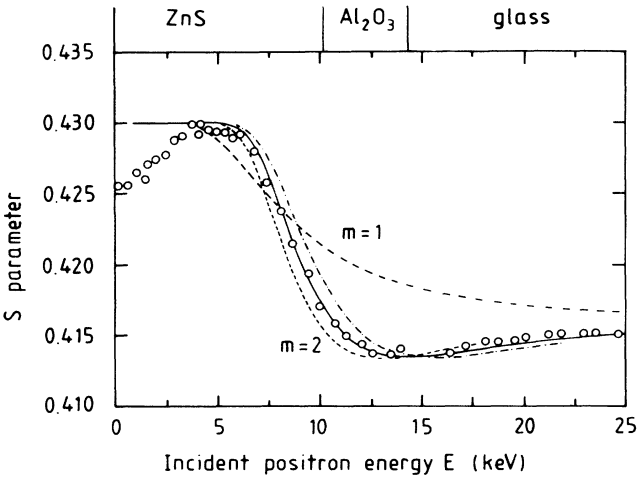

FIG. 3. Experimental and calculated $S(E)$ data in the sample with a 4000-Å ZnS/3000-Å Al_2O_3/glass structure. The three Gaussian ($m=2$) fits correspond to $n=1.65$ (dashed line), $n=1.60$ (solid line), and $n=1.55$ (dashed-dotted line).

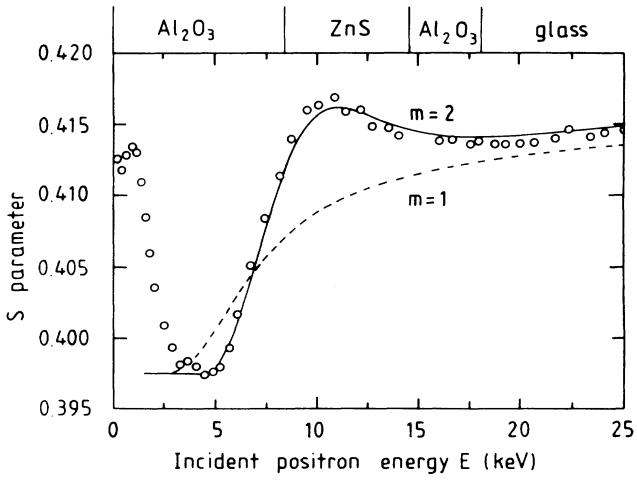

FIG. 4. Experimental and fitted $S(E)$ data in the 3000-Å Al_2O_3/4000 Å ZnS/3000 Å Al_2O_3/glass structure. All parameters in the fit are fixed to preceding values (with $n=1.6$). Energies, where the median positron penetration R crosses the interfaces, are shown in the upper horizontal axis.

median penetration depth $R=[3.8(3)\ \mu g/cm^2](E)^{1.62(5)}$. ($E$ in all these expressions is in units of keV.) We emphasize that only the last value can be directly compared with experimental transmission measurements.[17,18] Some examples of the positron implantation profiles calculated for the $Al_2O_3/ZnS/Al_2O_3$/glass structure, using the above parameters, are shown in Fig. 5.

Figures 2–4 can also be used to estimate the depth resolution of monoenergetic positrons to probe heterogeneous samples. In all cases the first interface at 3000 Å or 4000 Å is seen as an abrupt transition in S. In Fig. 4 the underlying ZnS layer is also fairly well evidenced by the maximum at $E=11$ keV. However, this is much less obvious if the layers have characteristic S values closer to each other, which is the case for the Al_2O_3/glass interface in Fig. 3. On the other hand, the Al_2O_3 layer in Fig. 4, located at 7000–10000 Å is still observable from the very shallow minimum around $E=18$ keV. To test depth resolution capabilities of our method, we reanalyzed the data with fixed ($\alpha=4.0\ \mu g/cm^2$, $m=2.0$, and $n=1.62$) implantation profile parameters, but floating the interface positions. The fit yields the three interface locations at depths 2950±50 Å, 7000±80 Å, and 10 300±150 Å, respectively. Within the accuracy of the direct thickness measurements, these values compare favorably with the nominal interface locations (3000, 7000, and 10 000 Å) shown in Fig. 1. Above, the error bars stand for statistical errors only. The goodness of the fit, especially for data shown in Fig. 4, also improves significantly, when interface positions are changed from the nominal values.

The measured positronium fraction f has virtually vanished at $E=1$ keV. Thus the $S(E)$ data between 1 and 5 keV can be directly used to estimate[23] the positron mobility in various layers. We note that the apparent diffusion parameter E_0 is still small, but it is larger (~ 1500 eV) than that deduced from Ps fraction measurements. The corresponding diffusion length[3,4] is $L_+ \sim 200$ Å. Therefore, the assumed low positron mobility leading to our data analysis is still valid, especially at high E, where the range of the positron implantation profile is very much higher than the diffusion length. From the two sets of measurements, we argue that the $S(E)$ data above $E=1$ keV are more appropriate to yield positron mobility information than the Ps fraction f at low incident energies E. The latter appears to be fully due to epithermal positrons[19–21] in the present system. As deduced from the $S(E)$ data in Figs. 2–4, the positron diffusion is rather weak in all layers, perhaps slightly weaker in Al_2O_3 than in ZnS. Thus it seems likely that a relatively high density of defects trapping positrons must exist in each layer, with a concentration[4,10] of order $10^{-4}, \ldots, 10^{-3}$.

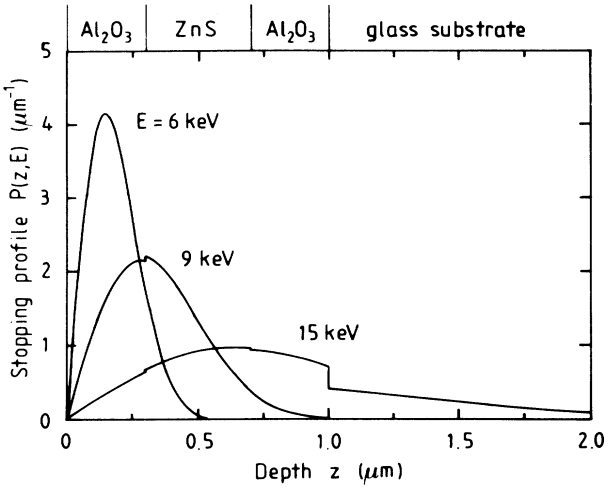

FIG. 5. Calculated positron implantation profiles $P(z,E)$ for various incident positron energies E in the $Al_2O_3/ZnS/Al_2O_3$/glass structure. No interference effects of the interfaces on the positron slowing-down properties is assumed. The discontinuities in $P(z,E)$ arise from changes in the layer densities ρ_i [see Eq. (1)].

V. CONCLUSIONS

In conclusion, we have studied a multilayer structure with monoenergetic positrons with varying incident energy E. The positron implantation profile was shown to possess a shape of a derivative of a Gaussian function [$m=2.0(1)$, Eq. (1)], at least for incident positron energies $E>4$ keV, in accordance with recent computer simulations. The mean implantation depth $\bar{z}$ is observed to be $\bar{z}=[4.0(3)\ \mu g/cm^3](E)^{1.62(5)}$. Probing heterogeneous samples can be accomplished with our technique at least down to depths of about 1 μm with a depth resolution of order 100 Å. Further experiments are needed to analyze capabilities of our method in systems where the positron mobility is significantly higher. Our Al_2O_3/ZnS heterostructure seems to contain a large concentration of open-volume defects capable of positron trapping.

ACKNOWLEDGMENT

We are grateful to Lohja Corporation for providing us with the sample and to E. Punkka for experimental assistance.

[1] *Positron Solid State Physics*, edited by W. Brandt and A. Dupasquier (North-Holland, Amsterdam, 1983).

[2] A. P. Mills, Jr., Science **218**, 335 (1982).

[3] A. P. Mills, Jr., in *Positron Solid State Physics*, Ref. 1, pp. 432–509.

[4] K. G. Lynn, in *Positron Solid State Physics*, Ref. 1, pp. 609–643.

[5] A. Vehanen, J. Mäkinen, P. Hautojärvi, H. Huomo, J. Lahtinen, R. M. Nieminen, and S. Valkealahti, Phys. Rev. B **32**, 7561 (1985); J. Mäkinen, A. Vehanen, P. Hautojärvi, H. Huomo, J. Lahtinen, R. M. Nieminen and S. Valkealahti, Surf. Sci. **175**, 385 (1986).

[6] M. D. Bentzon, H. Huomo, A. Vehanen, P. Hautojärvi, J. Lahtinen, and M. Hautala, J. Phys. F (to be published).

[7]W. Triftshäuser and G. Kögel, Phys. Rev. Lett. **48**, 1741 (1982).
[8]K. G. Lynn, D. M. Chen, B. Nielsen R. Pareja, and S. Myers, Phys. Rev. B **34**, 1449 (1986).
[9]S. Tanigawa, Y. Iwase, A. Uenodo, and H. Sakairi, J. Nucl. Mater. **133&134**, 463 (1985).
[10]A. Vehanen, K. G. Lynn, P. J. Schultz, E. Cartier, H.-J. Güntherodt, and D. M. Parkin, Phys. Rev. B **29**, 2371 (1984).
[11]Y. Iwase, A. Uenodo, and S. Tanigawa, in *Positron Annihilation,* edited by P. C. Jain, R. M. Singru, and K. P. Gopinathan (World-Scientific, Singapore, 1985), pp. 977–979.
[12]B. Nielsen, A. van Veen, and K. G. Lynn, in *Positron Annihilation,* edited by P. C. Jain, R. M. Singru, and K. P. Gopinathan (World-Scientific, Singapore, 1985), pp. 836–838.
[13]S. Valkealahti and R. M. Nieminen, Appl. Phys. A **32**, 95 (1983); **35**, 51 (1984).
[14]*Positrons in Solids,* edited by P. Hautojärvi, Vol. 12 of *Topics in Current Physics* (Springer, Berlin, 1979).
[15]J. Lahtinen, A. Vehanen, H. Huomo, J. Mäkinen, P. Huttunen, K. Rytsölä, P. Hautojärvi, and M. D. Bentzon, Nucl. Instrum. Methods B **17**, 73 (1986).
[16]V. P. Tanninen, M. Oikkonen, and T. Tuomi, Thin Solid Films **109**, 283 (1983).
[17]A. P. Mills, Jr. and R. J. Wilson, Phys. Rev. A **26**, 490 (1982).
[18]More rigorously, experimental values of α should be related to the *median* positron penetration depth R (see Ref. 17). For a Gaussian ($m=2$) profile, however, R and the mean depth $\bar{z}$ are very similar ($R=0.94\bar{z}$).
[19]B. Nielsen, K. G. Lynn, and Y.-C. Chen, Phys. Rev. Lett. **57**, 1789 (1986).
[20]R. H. Howell, I. J. Rosenberg, and M. J. Fluss, Phys. Rev. B **34**, 3069 (1986).
[21]H. Huomo, A. Vehanen, M. D. Bentzon, and P. Hautojärvi, Phys. Rev. B (to be published).
[22]B. Nielsen, K. G. Lynn, A. Vehanen, and P. J. Schultz, Phys. Rev. B **32**, 2296 (1985).
[23]Note that in the presence of a nonzero Ps fraction ($f>0$), the Doppler data $S(E)$ are no longer linear in terms of the positron probability $J=f(E)/f(0)$ to diffuse back to the surface. More details will be published separately.